

Application of Microplasma Noise Statistical Characteristics to Studying the PN Junction Heating in the Neighbourhood of Local Defects

M. RASKA, P. KOKTAVÝ

Department of Physics, Faculty of Electrical Engineering and Communication
Brno University of Technology
Technická 8, 616 00 Brno
CZECH REPUBLIC

xraska04@stud.feec.vutbr.cz, <http://www.ufyz.feec.vutbr.cz>

Abstract: Local avalanche breakdowns take place in the neighbourhood of PN junction local defects at sufficiently high reverse voltage. These breakdowns give rise to microplasma noise which is often characterized by current impulses whose inception time and duration time are random. The effective cross-section of the microplasma region being rather small, the current density may achieve a high value, which in turn can result in local heating of the micro-region and, consequently, the junction destruction. The present paper deals with the effect of the temperature on statistical characteristics of microplasma noise. This effect is intended to be used for the local defect temperature determination based on these characteristic measurement results.

Key-Words: Microplasma noise, PN junction, Avalanche breakdown, Statistical characteristic, Noise diagnostics

1 Introduction

Local avalanche breakdowns take place in the neighbourhood of PN junction local defects at sufficiently high reverse voltages. These breakdowns give rise to microplasma noise. The behaviour of this type of noise depends on the measuring circuit parameters [1]. We studied the statistical characteristics of this type of noise in a low-impedance circuit, the device being powered from a constant voltage source. In this case, the microplasma noise has the form of approximately rectangular impulses, the amplitude of which is constant, the impulse inception and duration being random [2].

Among the most important microplasma noise characteristics, there are the impulse duration distribution density and the neighbouring impulse separation distribution density. These quantities versus time plots show an exponential shape frequently [3]. However, our experiments showed certain deviations from the exponential curve, see Fig. 1. We attribute these deviations to a local temperature increase in the avalanche breakdown region during the impulse duration [4]. Whereas GaAsP LEDs and silicon solar cells showed rather small deviations within the time intervals measured (1 μ s to 1 ms), the deviations were considerably heavy in silicon rectifier diodes.

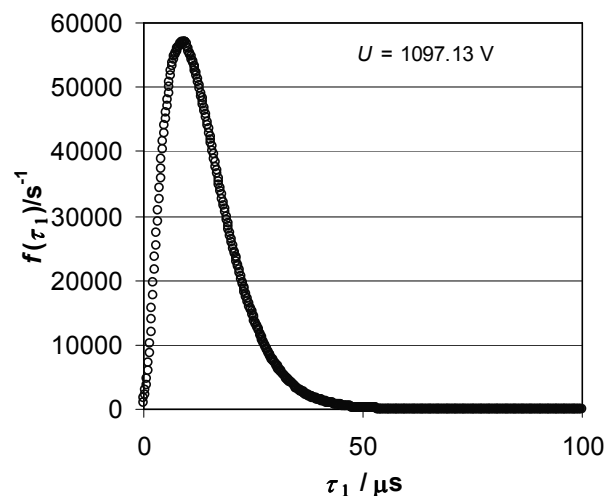


Fig. 1. Impulse duration probability distribution density, A04 specimen, $U_R = 1097.13$ V.

2 Microplasma Noise as a two-state Generation-Recombination Process

The experiments show that the microplasma bistable behaviour may be described with a two-state stochastic process of generation-recombination type (G-R process), which is Markovian, provided

that the diode power supply is a voltage source. Two postulates describe the primary process:

1. If the system is at a time t in the state 0 then the transition probability to the state 1 within the time interval $(t, t + \Delta t)$ equals $g \Delta t + o(\Delta t)$.
2. If the system is at a time t in the state 1 then the transition probability to the state 0 within the time interval $(t, t + \Delta t)$ equals $r \Delta t + o(\Delta t)$.

The quantities g and r are the respective generation and recombination coefficients, both depending on the applied voltage and temperature for stationary random processes and $o(\Delta t)$ is a term going to zero when Δt is going to zero.

In what follows we will only deal with the impulse duration statistical characteristics, which are determined by the recombination coefficient r , according to the 2nd postulate.

Let $P_1^-(t)$ denotes the probability of the impulse being not terminated within the time interval $(0, t)$. If this is the case, it will hold

$$P_1^-(t + \Delta t) = (1 - r\Delta t)P_1^-(t). \quad (1)$$

A differential equation can be derived from (1) as follows

$$\frac{dP_1^-(t)}{dt} = -rP_1^-(t). \quad (2)$$

Assuming the coefficient r to be constant throughout the impulse duration, the solution of (2) may be expressed in the following form

$$P_1^-(t) = Ce^{-rt}, \quad (3)$$

where C is a constant.

From the initial condition

$$P_1^-(0) = 1 \quad (4)$$

it follows that $C = 1$, hence

$$P_1^-(t) = e^{-rt}. \quad (5)$$

Considering the impulse duration τ_1 to be a random quantity, the distribution function of this random quantity will be

$$F(\tau_1) = P\{t \leq \tau_1\} = 1 - P_1^-(\tau_1) = 1 - e^{-r\tau_1}. \quad (6)$$

The probability distribution density of the random quantity τ_1 is

$$f(\tau_1) = \frac{dF(\tau_1)}{d\tau_1} = re^{-r\tau_1}. \quad (7)$$

If the recombination coefficient depends on the time in the course of the impulse duration, the equation (2) must be solved with a particular $r(t)$ function to determine the distribution function and the probability density distribution function. It holds

$$\frac{dP_1^-(t)}{dt} = -r(t)P_1^-(t). \quad (8)$$

Assuming the coefficient $r(t)$ not to be constant throughout the impulse duration, the solution of (8) may be expressed in the following form

$$P_1^-(t) = Ce^{-\int r(t)dt}. \quad (9)$$

From the initial condition

$$P_1^-(0) = 1 \quad (10)$$

it follows again that $C = 1$, hence

$$P_1^-(t) = e^{-\int r(t)dt}. \quad (11)$$

The distribution function of the impulse duration τ_1 will be

$$F(\tau_1) = P\{t \leq \tau_1\} = 1 - P_1^-(\tau_1) = 1 - e^{-\int r(\tau_1)d\tau_1}. \quad (12)$$

The probability distribution density of the random quantity τ_1 is

$$f(\tau_1) = \frac{dF(\tau_1)}{d\tau_1} = r(\tau_1)e^{-\int r(\tau_1)d\tau_1}. \quad (13)$$

3 Recombination Coefficient Temperature Dependence

If a local heating occurs during the avalanche discharge in the microplasma region, the recombination coefficient versus temperature plot is rather difficult to determine. Fortunately, the shape of this plot can be found out. We are referring to paper [3], which dealt with an experimental study of GaAsP LED microplasma noise statistical characteristics and the temperature dependence of these characteristics. It follows from the results presented in the mentioned paper, see Fig. 2, that the recombination coefficient versus temperature plot is exponential within 20° C – 40° C, as follows

$$r(T) = ae^{bT}, \quad (14)$$

where $a > 0$ and $b > 0$ are constants.

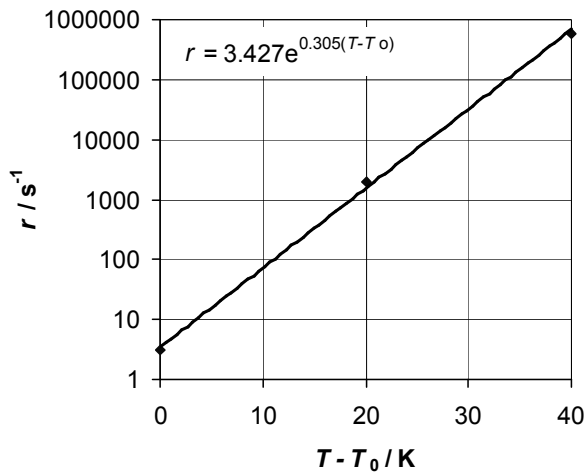


Fig. 2. Recombination coefficient versus temperature, M10 specimen, $U_R = 21.4$ V, $T_0 = 293$ K.

4 Current pulse waveform during a local breakdown

The microplasma noise has a form of rectangular current pulses frequently, but it can be changed due to local heating inside the discharge region [4]. Considerable deviations from the rectangular pulses were found out in silicon diodes after the influence of the measuring circuit on the pulse waveform had been eliminated. Paper [5] shows that the pulse shape is related to the discharge region local heating in these devices. Fig 3 shows a pulse which results

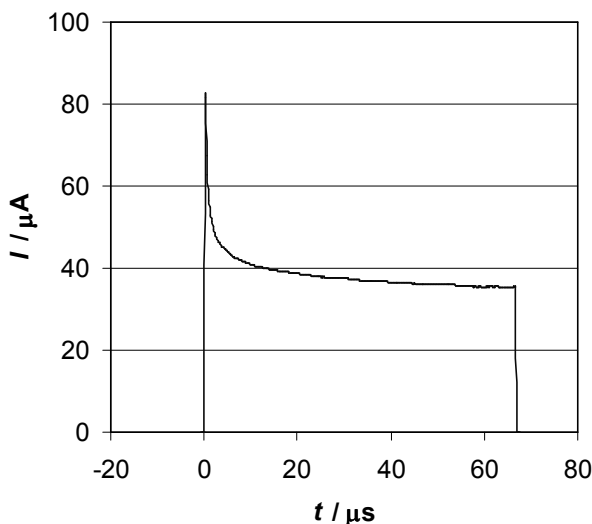


Fig. 3. Current pulse waveform for a local avalanche breakdown.

from averaging a great number of measured pulses (~500), which follow each other after a sufficiently

long time interval (>120 μs). This time interval is intended to allow the discharge region to cool down. Based on thus obtained waveform, the electric power supplied to the discharge region during the local discharge can be determined.

5 Heat Generated in the Microplasma Region

Let us assume that a certain amount of heat arises in a microplasma local region during the local avalanche breakdown. This amount of heat is supposed to be dissipated in the surrounding homogeneous material. The temperature will go up in the discharge region within the impulse duration. This process is described by the following heat conduction equation

$$\frac{\partial T}{\partial t} = \frac{\lambda}{\rho_m c} \nabla^2 T + \frac{w}{\rho_m c}, \quad (15)$$

where T is the temperature looked for, t is the time, λ is the specific thermal conductivity, ρ_m is the density, c is the specific thermal capacity and w is the heat source power density. It holds for silicon: $\lambda = 149 \text{ W.m}^{-1}.\text{K}^{-1}$, $\rho_m = 2330 \text{ kg.m}^{-3}$, $c = 703 \text{ J.kg}^{-1}.\text{K}^{-1}$.

If the discharge region can be considered to be spherical it is advisable to transform this equation into spherical coordinates:

$$\frac{\partial T}{\partial t} = \frac{\lambda}{\rho_m c} \left(\frac{\partial^2 T}{\partial \rho^2} + \frac{2}{\rho} \frac{\partial T}{\partial \rho} \right) + \frac{w}{\rho_m c}, \quad (16)$$

where ρ is the distance from the discharge region centre.

Numerical solution of (16) resulted in heating centre temperature versus time plots for different heating region sizes (radius ρ_0) is shown in Fig. 4. It was assumed here that the whole energy supplied transforms into heat which is generated uniformly throughout the heating region. The power input can be expressed as

$$P_i = U_R i, \quad (17)$$

where $U_R = 1097.13$ V is a reverse voltage applied to the junction and $i(t)$ is the pulse current (see Fig 3). Consequently, the power density in a spherical heating region of radius ρ_0 will be

$$w = \frac{P_i}{\frac{4}{3}\pi\rho_0^3}. \quad (18)$$

Furthermore, the initial temperature is supposed to be $T_0 = 0$ at a point in space. The calculation was carried out for a spherical silicon specimen of radius of 1 mm, which corresponds to the size of Si diodes under investigation.

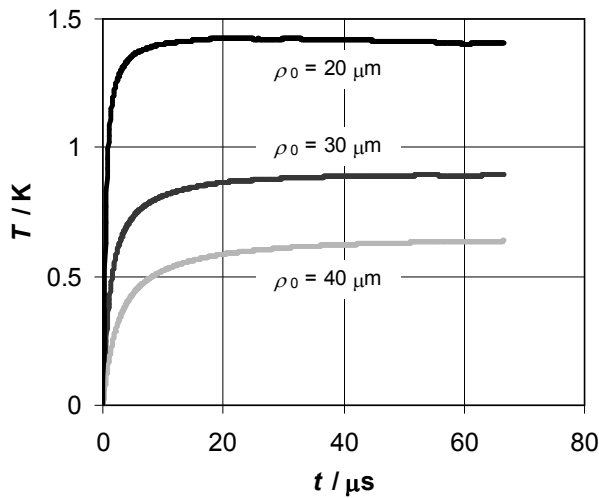


Fig. 4. Examples of the temperature vs. time plots for the microplasma region centre, numerical solution, homogeneous silicon.

Logarithmic scale was used for the time axis of the temperature vs. time plot for better depiction, see Fig. 5.

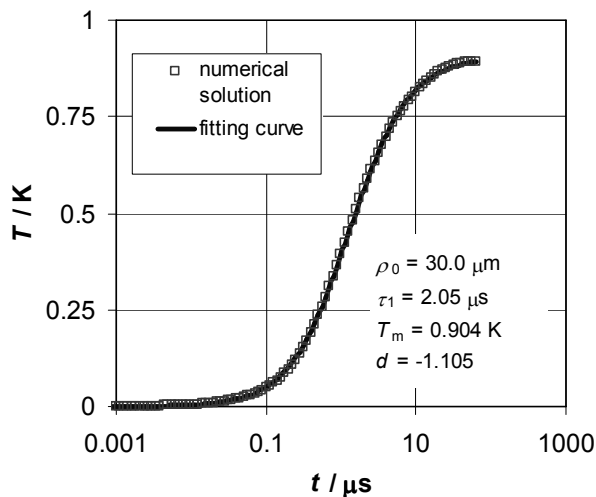


Fig. 5. Numerical solution and fitting of the temperature time dependence for the heating region centre, homogeneous silicon.

Following function has been suggested for an analytical representation of the curves obtained

$$T = \frac{T_m}{(t/\tau_{th})^d + 1}, \quad (19)$$

where $T_m > 0$, $\tau_{th} > 0$ and $d < 0$ are the parameters we obtained by approximating the different solutions. Here, T_m is the maximum temperature achieved after a sufficiently long time and the time constant τ_{th} expresses the time at which the temperature equals $T_m/2$. Fig. 5 makes it clear that there is a good agreement between the numerical solution and the analytical representation function.

As the only parameter to determine the temperature behaviour at the centre of the heating region is the radius of this region, ρ_0 , Fig. 6 shows

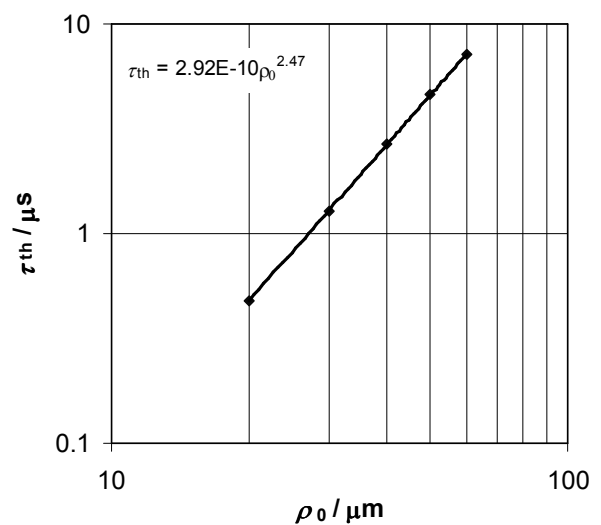


Fig. 6. Heating zone centre temperature growth time constant versus heat generation region radius plot, $U_R = 1097.13$ V.

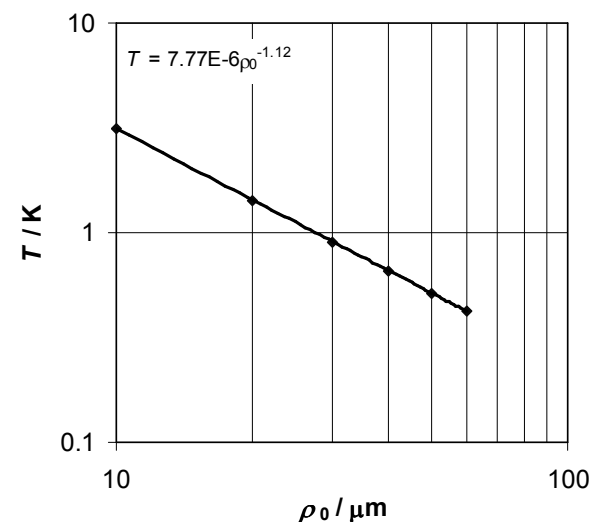


Fig. 7. Heating zone centre maximum temperature versus heat generation region radius plot, $U_R = 1097.13$ V

the temperature growth time constant versus region radius plot and Fig. 7 shows the maximum temperature at the heated region centre versus region radius plot (obtained by a numerical calculation).

Fig. 8 shows the temperature behaviour as a function of the distance from the heating zone centre in the material under investigation at $t = 1 \mu\text{s}$ and $t = 66 \mu\text{s}$. It is evident that for a single pulse of the above duration, the whole amount of heat generated remains localized inside the material and the silicon-to-environment initial conditions have no effect on the resulting temperature behaviour at the region centre.

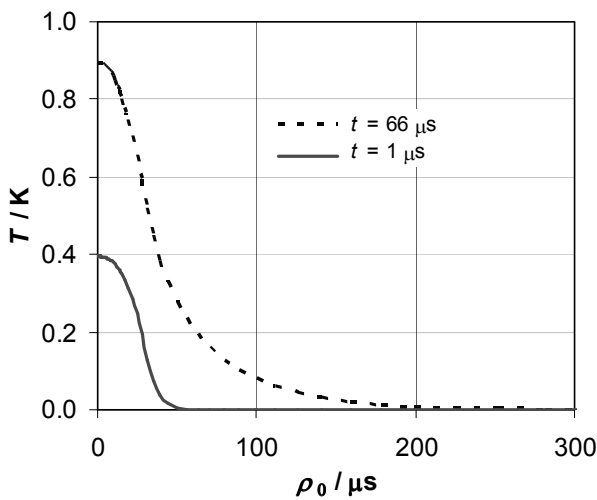


Fig. 8. Temperature versus distance from the discharge centre plot at $t = 1 \mu\text{s}$ and $t = 66 \mu\text{s}$.

Quite a different situation may arise if the silicon region is exposed to high-repetition-rate long-duration current pulses or, if the local discharge region is permanently ionised in a device to which a sufficiently high reverse voltage has been applied. In this case, global heating of the whole device may take place and heat dissipation from the device surface to the environment will play the role.

6 Recombination Coefficient versus Time Plot during the Recombination Process

The experimental impulse duration probability distribution density $f(\tau_1)$ being determined, the recombination coefficient versus time plot during the impulse being ON can be found. It holds for the distribution function:

$$F(\tau_1) = \int f(\tau_1) d\tau_1. \quad (20)$$

The probability of the impulse being not terminated within the time interval $(0, \tau_1)$ will follow from equation (6):

$$P_1^-(\tau_1) = 1 - F(\tau_1). \quad (21)$$

According to Equation (8) it holds

$$r(t) = -\frac{1}{P_1^-(t)} \frac{dP_1^-(t)}{dt}. \quad (22)$$

Combining equations (20), (21) and (22), we get an expression for the recombination coefficient:

$$r(t) = \frac{1}{1 - \int f(t) dt} f(t). \quad (23)$$

The recombination coefficient versus time plot as determined from the experimental impulse duration probability distribution density (Fig. 1) using equation (23) is shown in Fig. 9. We can see that the recombination coefficient grows with the time, which is in a good agreement with the temperature dependence and the local avalanche breakdown mechanism hypothesis. The recombination coefficient curve shown in log-log scale (Fig. 9) corresponds in shape to the region centre temperature behaviour of Fig. 4, which in turn justifies the application of formula (14) for the recombination coefficient temperature dependence. This is why equations (14) and (19) can be used to express the time dependence of the recombination coefficient during the impulse ON-state

$$r(t) = a \exp\left(\frac{bT_m}{(t/\tau_{th})^d + 1}\right). \quad (24)$$

Approximation of the experimental recombination coefficient versus time plot by function (24) is shown in Fig. 9. The suggested function is seen to fit the experiment results very well. This in turn confirms the correctness of our hypothesis concerning the local heating effect on the microplasma noise statistical characteristics.

The best-fit procedure results in the values of quantities a , bT_m , τ_{th} and d .

Based on thus obtained time constant $\tau_{th} = 2.05 \mu\text{s}$ and using Fig. 6, the assumed radius of the region can be determined, equalling $\rho_0 = 36.1 \mu\text{m}$. Furthermore, from Fig. 7, the maximum temperature at the region centre can be read out to be $T_m = 0.741 \text{ K}$.

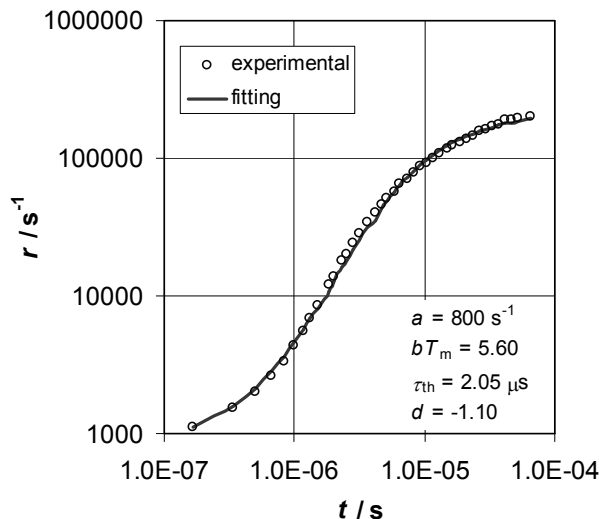


Fig. 9. Recombination coefficient vs. time plots, specimen A04.

7 Conclusion

Based on our analysis of the statistical generation-recombination process for a time-dependent recombination coefficient in the course of the pulse duration, an algorithm for determining the recombination coefficient time dependence from the experimental pulse duration probability density distribution has been found out. In this way, it was verified that the experimentally determined changes in the impulse duration distribution density can be due to the recombination coefficient time dependence.

Based on the modelling of the conduction of the heat generated in the avalanche discharge local region and using the recombination coefficient experimental temperature dependence function, a function $r(t)$ has been put forward. The proposed theoretical curves have proved to be in a very good agreement with the experimental curves, confirming the correctness of our hypothesis.

Fitting the experimental curves of the recombination coefficient time dependence with the theoretical function resulted in the parameter values characterizing the given waveform. Using these parameter values, a numerical calculation of the heating region centre temperature behaviour was carried out to give the maximum temperature $T_m = 0.741$ K above the room temperature and the discharge region size $\rho_0 = 36.1$ μm . Thus obtained maximum temperature attained places the device in no jeopardy at all. It is to be noted, however, that the calculation has been carried out for a single pulse only. If long-duration, high-repetition-rate pulses are applied to the device or, if a permanently ionized

channel arises in the device, the temperature may achieve substantially higher values after a sufficiently long time. Another temperature increase at the region centre could be due to a non-uniform heat generation inside the region. Furthermore, it is to be stated that the calculated size of the local region in which heat is generated, can, in general, differ from the size of the discharge region of the local avalanche breakdown in the defect neighbourhood.

The results of this research are applicable to the diagnosis of PN junction local defects.

Acknowledgements

This paper is based on the research supported by the Grant Agency of the Czech Republic, grant No. 102/06/1551 and project VZ MSM 0021630503.

References

- [1] Champlin, KS. Microplasma Fluctuations in Silicon. *J. Appl. Phys.*, July 1959, vol. 30, no. 7, p. 1039-1050.
- [2] Haitz, RH. Model for the Electrical Behavior of Microplasma. *J. Appl. Phys.*, May 1964, vol. 35, no. 5, p. 1370-1376.
- [3] Koktavý, P., Šikula, J. Reverse Biased P-N Junction Noise in GaAsP Diodes with Avalanche Breakdown Induced Microplasmas. *Fluctuation and Noise Letters*, 2002, Vol. 2, No 2, p. L65 – L70.
- [4] McINTYRE, RJ. Theory of Microplasma Instability in Silicon. *J. Appl. Phys.*, June 1961, vol. 32, no. 4, p. 983-995.
- [5] Raška, M., Koktavý, P., Andreev, A. *Determination of temperature in microplasma region*. In *New Trends in Physics*. Brno, Czech Republic, 2007. p. 122-125.